# Statistical characterization of air ion mobility spectra at Tahkuse Observatory: Classification of air ions

U. Hõrrak, J. Salm, and H. Tammet
Institute of Environmental Physics, University of Tartu, Tartu, Estonia

**Abstract.** A database of 8615 hourly averaged air ion mobility spectra in the range of 0.00041–3.2 $cm^2 V^{-1} s^{-1}$ was measured at Tahkuse Observatory, Estonia, during 14 months in 1993–1994. The average mobility spectrum over the whole period shows distinct peaks of small and large ions. Intermediate ions with mobilities of 0.034–0.5 $cm^2 V^{-1} s^{-1}$ are of low concentration of about 50 $cm^{-3}$ in the average spectrum. They experience occasional bursts of up to about 900 $cm^{-3}$ during 6–10 hours at daytime. The number of burst events recorded during 14 months was 101, with maximum frequency in spring and minimum frequency in winter. Physically, large and intermediate ions can be called aerosol ions, and small ions can be called cluster ions. The principal component analysis was applied to detect the structure of an air ion mobility spectrum. As a result, the mobility spectrum in the range of 0.00041–3.2 $cm^2 V^{-1} s^{-1}$ (diameters of 0.36–79 nm) was divided into five classes: small cluster, big cluster, intermediate, light large, and heavy large ions. The boundaries between the classes are 1.3 $cm^2 V^{-1} s^{-1}$ (diameter of 0.85 nm), 0.5 $cm^2 V^{-1} s^{-1}$ (1.6 nm), 0.034 $cm^2 V^{-1} s^{-1}$ (7.4 nm), and 0.0042 $cm^2 V^{-1} s^{-1}$ (22 nm). The five principal components that are closely correlated with the respective ion classes explain 92% of total variance. The classification of aerosol ions is in accord with the three-modal structure of the size spectrum of submicron aerosol particles.

## 1. Introduction

Measurements of the mobility spectra of natural air ions could be most generally characterized by the mobility range and resolution and by the frequency and duration of recordings. In various papers, these characteristics have varied to a large extent, depending on particular goals and technical resources of the researchers. The spectrometer designed by Misaki [1961a] has a high resolution of eight logarithmically divided fractions per decade of mobility. At first the spectra of small ions in the range of 0.2–3 $cm^2 V^{-1} s^{-1}$ were measured at two different sites in Japan during a few days [Misaki, 1961b]. Later the spectra of large ions in the range of 0.00018–0.01 $cm^2 V^{-1} s^{-1}$ (11 days) and in the range of 0.000042–0.0024 $cm^2 V^{-1} s^{-1}$ (3 days) were measured in the New Mexico semidesert in 1963 [Misaki, 1964]. Thereafter measurements in the wide range of 0.0001–3.2 $cm^2 V^{-1} s^{-1}$ were carried out at three sites in Japan; the whole duration of the measurements was about 1 month [Misaki et al., 1972]. Kojima [1984] measured air ion mobility spectra in the range of 0.0085–0.24 $cm^2 V^{-1} s^{-1}$. Five series (7–10 days) of measurements were carried out at the campus of the Science University of Tokyo in Noda during three seasons from summer 1983 to spring 1984. Dhanorkar and Kamra [1991, 1993a] designed and built a mobility spectrometer with three measuring condensers that covers a range of 0.00023–3.4 $cm^2 V^{-1} s^{-1}$. They recorded 28 spectra (6 spectra a day) at Pune, India, in 1991 [Dhanorkar and Kamra, 1993a]. The concentrations of small, intermediate, and large ions were recorded at the same place during nearly 1 year in 1990–1991 [Dhanorkar and Kamra, 1993b].

Owing to the complexity and large-scale variability of atmospheric processes, episodic measurements are not sufficient to characterize the regularities of the mobility spectra of natural air ions. Long-term measurements of air ions in a wide range of mobility are necessary to draw statistically founded conclusions about the shape and variations of the mobility spectra for periods of different duration.

The classification of air ions represents one essential problem that can be studied by long-term measurements of air ion spectra. The classification has been established gradually [Israël, 1970; Flagan, 1998], but it has not been satisfactorily formulated until now. The concepts of small and large ions have a clear physical background [Tammet, 1995]. Problems arise when trying to specify the concept of intermediate ions and settle the mobility boundaries. The boundaries defined in atmospheric electricity textbooks are rather speculative conventions. One way of development is the statistical analysis of the air ion spectra measured in a wide mobility range, in order to search for air ion groups with different statistical properties. A natural classification should explain the coherent behavior of air ions inside class intervals and the relative independence of the ions of different classes. Measurements used in the verification of the

classification are required to record air ion mobility fractions that are narrow in comparison with mobility classes. The analysis of the statistical behavior of fraction concentrations requires thousands of mobility spectra recorded during at least one full year. The first measurements that allow statistical classification of air ions were carried out at Tahkuse Observatory.

The measurement of detailed mobility spectra in natural atmospheric air at Tahkuse Observatory has been running since 1985. The mobility spectrum of small air ions together with a narrow fraction of light intermediate ions was measured from June 1985 to June 1986 [Hõrrak et al., 1988]. Instrumentation for measurements in a wide mobility range was set into operation in July 1988. A brief summary of measurements for the period until 1989 was reported by Hõrrak et al. [1994]. A description of the behavior of intermediate ions at Tahkuse Observatory for the period from September 1993 to October 1994 was presented by Hõrrak et al. [1998b]. A statistical synopsis of the air ion spectra for the entire mobility range at the same place and for the same period is given in the present paper, with emphasis on the study of air ion classification. The large and intermediate ions are charged aerosol particles. Thus the problem is related to the size classification of atmospheric aerosol particles.

## 2. Measurements

### 2.1. Location

Tahkuse Observatory with coordinates 58°31'N, 24°56'E is located in a sparsely populated rural region. It is 27 km northeast of the city of Pärnu and 100 km south of Tallinn, the capital of Estonia. Pärnu, with 52,000 inhabitants, is located on the coast of the Gulf of Riga, at the east coast of the Baltic Sea. The terrain surrounding the observatory consists of flat open country with some tree groups (about 100 trees in a radius of 100 m), small woods, grassland, and agricultural land. The river of Pärnu is 50 m to the northwest; the nearest neighboring farm is about 200 m west. A road with little automobile traffic passes about 180 m east from the measurement point. The average traffic frequency was about 10 motor vehicles per day, mainly from 0700 to 1900 local standard time (LST), in 1993–1994. The Soomaa National Park (Swampland) extends at distances from 6 to 30 km southeast. The weather in this region is quite unsteady owing to the action of cyclones and anticyclones.

### 2.2. Instrumentation

A complex of air ion spectrometers covering a mobility range of 0.00041–3.2 $cm^2\ V^{-1}\ s^{-1}$ was installed at Tahkuse in 1988 [Hõrrak et al., 1990; Tammet, 1990]. The upper mobility limit was chosen to collect the smallest existing air ions. The lower mobility limit is determined by the technical parameters of the equipment. The complex consists of three original multichannel aspiration spectrometers designed according to the principle of the second-order differential mobility analyzer [Tammet, 1970]. The spectrometers are by convention called small ion spectrometer ($IS_1$), intermediate ion spectrometer ($IS_2$), and large ion spectrometer ($IS_3$). The illustration of the $IS_1$ and the measuring system is presented in Figure 1.

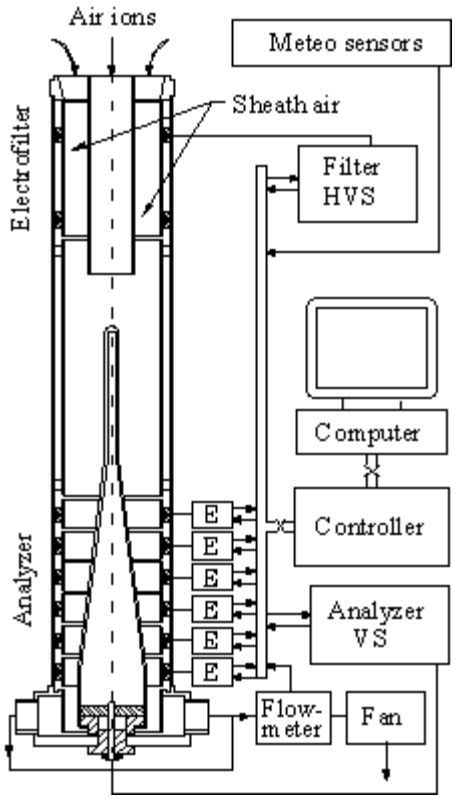


Figure 1. Small air ion spectrometer $IS_1$ and the measuring system. E, electrometer amplifier; HVS, high-voltage supply; and VS, voltage supply. External dimensions of the spectrometer: height, 695 mm; diameter, 122 mm.

The design of the $IS_2$ and $IS_3$ is analogous. The whole range of mobility is logarithmically divided into 20 intervals (see Table 1): 9 intervals in the subrange of 0.00041–0.29 $cm^2\ V^{-1}\ s^{-1}$ and 11 intervals in the subrange of 0.25–3.2 $cm^2\ V^{-1}\ s^{-1}$. Thus each mobility spectrum consists of 20 fraction concentrations. The symbols of fractions are $N_k$ and $P_k$ for negative and positive polarity, respectively. The whole mobility range of intermediate ions is covered by means of two spectrometers ($IS_1$ and $IS_2$) of different resolving power. Accordingly, the measured logarithmically distributed fractions of heavy intermediate ions (12–13) are about 3 times wider than those of light intermediate ions (fractions 9–11). The eleventh fraction (0.251–0.320 $cm^2\ V^{-1}\ s^{-1}$) is overlapped by the twelfth fraction (0.150–0.293 $cm^2\ V^{-1}\ s^{-1}$).

The mobility spectra of positive and negative air ions were measured every 5 min. The hourly averages and standard deviations of air ion fraction concentration inside the hourly periods were recorded together with the values of wind direction, wind speed, atmospheric pressure, temperature, relative humidity, and the concentration of $NO_2$.

The air is sucked into the mobility spectrometers through an opening in the south gable of the building at a height of about 5 m from the ground. To prevent the effect of wind to the airflow, the air inlet (above) and outlet (beneath the inlet) are placed in the same gable with a space of about 1 m. The length of aluminum tube that conducts the air sample to the spectrometers is about 2 m, with a crosssection of 18 ´ 20 $cm^2$. There are thin longitudinal metal sheets in the tube for suppression of turbulence. The total air flow rate is about 0.016 $m^3\ s^{-1}$, and air speed is about 0.45 m $s^{-1}$. The devices, excluding meteorological sensors, are enclosed in a thermally insulated stable-climate chamber, which makes it possible to use the equipment through all the seasons. The chamber and the tube of the air channel are electrically earthed.

Table 1. Air Ion Fractions, Estimates of Equivalent Diameter Ranges Assuming Single Charged Particles, and Proposed Classes of Air Ions

| Analyzer | Fraction | Mobility$cm^2\ V^{-1}\ s^{-1}$ | Diameter |
|---|---|---|---|

| | | | nm |
|---|---|---|---|
| | | Small Cluster Ions | |
| $IS_1$ | $N_1/P_1$ | 2.51–3.14 | 0.36–0.45 |
| $IS_1$ | $N_2/P_2$ | 2.01–2.51 | 0.45–0.56 |
| $IS_1$ | $N_3/P_3$ | 1.60–2.01 | 0.56–0.70 |
| $IS_1$ | $N_4/P_4$ | 1.28–1.60 | 0.70–0.85 |
| | | Big Cluster Ions | |
| $IS_1$ | $N_5/P_5$ | 1.02–1.28 | 0.85–1.03 |
| $IS_1$ | $N_6/P_6$ | 0.79–1.02 | 1.03–1.24 |
| $IS_1$ | $N_7/P_7$ | 0.63–0.79 | 1.24–1.42 |
| $IS_1$ | $N_8/P_8$ | 0.50–0.63 | 1.42–1.60 |
| | | Intermediate Ions | |
| $IS_1$ | $N_9/P_9$ | 0.40–0.50 | 1.6–1.8 |
| $IS_1$ | $N_{10}/P_{10}$ | 0.32–0.40 | 1.8–2.0 |
| $IS_1$ | $N_{11}/P_{11}$ | 0.25–0.32 | 2.0–2.3 |
| $IS_2$ | $N_{12}/P_{12}$ | 0.150–0.293 | 2.1–3.2 |
| $IS_2$ | $N_{13}/P_{13}$ | 0.074–0.150 | 3.2–4.8 |
| | | Light Large Ions | |
| $IS_2$ | $N_{14}/P_{14}$ | 0.034–0.074 | 4.8–7.4 |
| $IS_2$ | $N_{15}/P_{15}$ | 0.016–0.034 | 7.4–11.0 |
| $IS_3$ | $N_{16}/P_{16}$ | 0.0091–0.0205 | 9.7–14.8 |
| $IS_3$ | $N_{17}/P_{17}$ | 0.0042–0.0091 | 15–22 |
| | | Heavy Large Ions | |
| $IS_3$ | $N_{18}/P_{18}$ | 0.00192–0.00420 | 22–34 |
| $IS_3$ | $N_{19}/P_{19}$ | 0.00087–0.00192 | 34–52 |
| $IS_3$ | $N_{20}/P_{20}$ | 0.00041–0.00087 | 52–79 |

### 2.3. Database

The present paper is based on data collected during the period from September 1, 1993, to October 27, 1994. The period under analysis involves 10,224 hours. Owing to occasional pauses in measurements and instrumentation failures, about 16% of the possible measuring time was lost, and 8615 hourly mobility spectra of both signs are available for statistical analysis. The computer program Statistica for Windows (Statsoft Inc., 1998) was used for statistical data analysis. A specific Pascal program was compiled for the principal component and factor analysis. The recorded air ion mobility fractions and estimates of the equivalent diameter ranges of air ion mobility assuming single charged particles [Tammet, 1995, 1998] are presented in Table 1. Five classes of air ions established by means of statistical analysis are also given.

A simplified method for the calculation of fraction concentrations, which does not take into account the shape of apparatus function, was applied in most sections of this paper.

The average spectra in Figure 2 were obtained in a stricter way by calculating first the parameters of a piecewise linear spectrum model [Tammet, 1980]. The simplified method yields somewhat smoothed mobility spectra. However, the differences, as compared to the stricter method, are small; uncertainties not exceeding a few percent are expected for fraction concentrations [Tammet et al., 1987]. The corrections of the diffusion losses of air ions on the entrance channel parts of spectrometers have been made by relevant equations [Tammet, 1970]. The correction factors are $1/(1 - 0.2k^{0.67})$ and $1/(1 - 0.08k^{0.67})$, where k is the mobility of ions, for spectrometer $IS_1$ and for $IS_2$+$IS_3$, respectively.

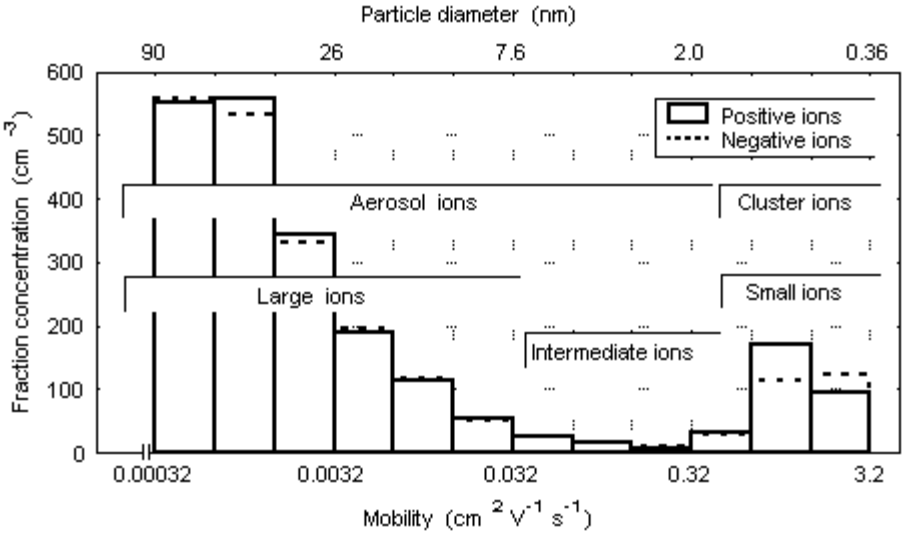


Figure 2. Average mobility spectra of air ions at Tahkuse Observatory, September 1, 1993, to October 27, 1994.

## 3. Results and Discussion

### 3.1. Mobility Spectrum of Air Ions

***3.1.1. Average spectra.*** The average mobility spectra of air ions for the whole period are presented in Figure 2. There are two wide spectral groups with the mobility ranges of 0.5–3.2 and 0.00032–0.034 $cm^2\ V^{-1}\ s^{-1}$, which are traditionally called small ions and large ions, respectively. More detailed average spectra of small ions are presented in Figure 3.

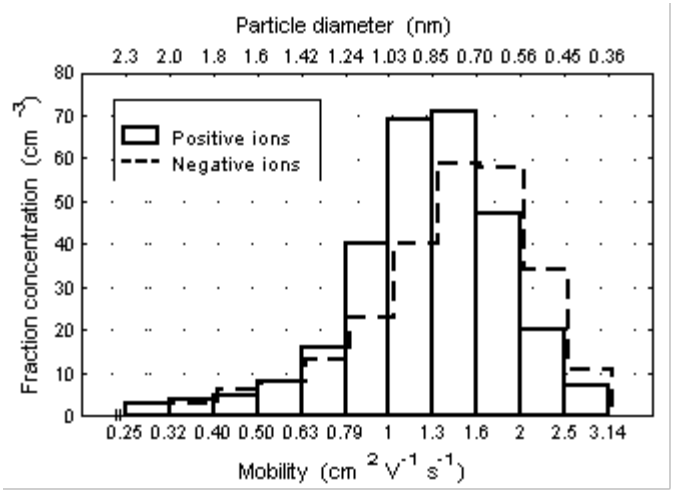


Figure 3. Average spectra of small (cluster) ions at Tahkuse Observatory, September 1, 1993, to October 27, 1994.

The corresponding particle diameters, derived from the electrical mobilities, are presented in the figures assuming single charged particles [Tammet, 1995]. The third group lies between large and small ions, with the mobility range of 0.034–0.5 $cm^2\ V^{-1}\ s^{-1}$, and is called intermediate ions. This group appears from time to time as burst events, occasionally occurring around local noon, and its average concentration is about 50 $cm^{-3}$. Physically, large and intermediate ions may be called aerosol ions, and small ions may be called cluster ions [Hõrrak et al., 1994].

The general shape of the mobility spectra of negative and positive small ions is astonishingly similar to that observed

by Misaki [1976], whose modes of small ion mobility spectra, 1.56 $cm^2 V^{-1} s^{-1}$ and 1.26 $cm^2 V^{-1} s^{-1}$, are close to those presented in Figure 3. Small (cluster) ions are formed in charged state and evolved via ion-molecule reactions in the atmosphere before they obtain their final size [Mohnen, 1977; Luts and Salm, 1994; Luts, 1995; Nagato and Ogawa, 1998]. The growth of small ions is thermodynamically hindered at a mobility of 0.5 $cm^2 V^{-1} s^{-1}$ (1.6 nm) in ordinary conditions.

The overall shape of the average spectra in the range of large ions (aerosol ions) is in accord with calculations based on the theory of bipolar charging of aerosol particles by small air ions [Salm, 1988; Hõrrak et al., 1998a]. The concentration of large ions diminishes toward higher mobilities owing to the reduction of charging probability and the concentration of aerosol particles. The lower boundary of the spectrum at a mobility of 0.00032 $cm^2 V^{-1} s^{-1}$ is determined by technical limitations of the spectrometer $IS_3$.

The time variations of the air ion mobility spectrum and the aerosol particle size spectrum are well correlated in a size range of 10–80 nm. The correlation coefficient varies from 0.91 to 0.97, depending on the size fraction. These aerosol particles in weakly polluted rural air are believed to be in a quasi-steady charging state [Hõrrak et al., 1998c].

The electrical state of aerosol particles in the intermediate ion range (nanometer particles) is not well known in natural atmosphere. The estimates of charging probability obtained by theoretical considerations and laboratory experiments vary from about 0.5% to 5% for particles from 2 to 10 nm, respectively [Hoppel and Frick, 1986; Reischl et al., 1996]. Experimental investigation of competitive ion-induced and binary homogeneous nucleation in gas mixtures shows that the above values may be greatly modified when ions are involved in the nucleation process [Kim et al., 1997, 1998].

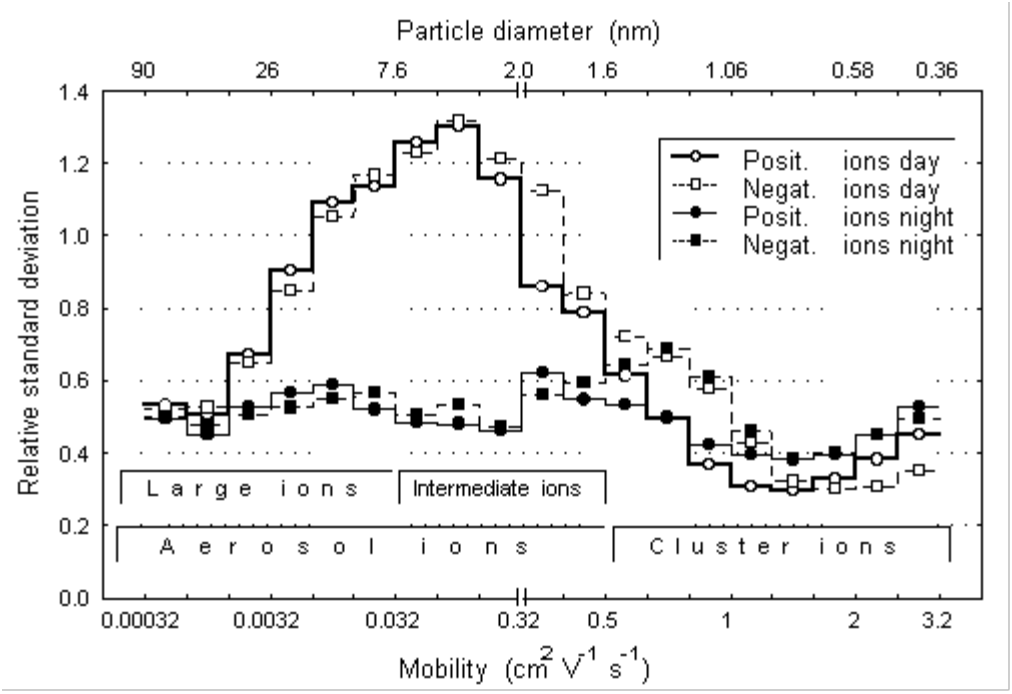


Figure 4. Relative standard deviations of the concentration of air ion spectral fractions at daytime (0700 to 2000 LST) and in the nighttime (2000–0700 LST) at Tahkuse Observatory, September 1, 1993, to October 27, 1994.

***3.1.2. Variability of spectra.*** The relative standard deviation (coefficient of variation) of the hourly averaged values of fraction concentrations is about 50% for small (cluster) air ions and 70% for large air ions. The average fraction concentrations of intermediate ions are relatively low, but their standard deviations are high, up to 130%, owing to the burst events with concentrations up to 900 $cm^{-3}$ [Hõrrak et al., 1998b]. The enhanced concentrations of intermediate ions are recorded from 1000 to 1900 LST, with a duration of 6–10 hours, in fine weather conditions. The relative standard deviations of the fractions of air ion mobility spectra in the daytime (0800–2000 LST) and nighttime (2000–0800 LST) are presented separately in Figure 4. A change of scale is set at a mobility of 0.32 $cm^2 V^{-1} s^{-1}$, according to

technical limitations of the spectrometers, and for better resolution of the spectral regions of aerosol ions and cluster ions.

Considering the whole data set, the relative standard deviation is close to the maximum values depicted in Figure 4 (in the case of large and intermediate ions close to that of daytime, and in the case of small ions, close to that of nighttime values). The crossing point of the curves for daytime and nighttime, at a mobility of about 0.5 $cm^2 V^{-1} s^{-1}$ (1.6 nm) in Figure 4, is in accordance with the boundary between cluster ions and aerosol ions [Tammet, 1995]. The above estimates of the relative standard deviations are equally valid for the large and intermediate air ion concentrations of both polarities, taking into account the random measuring errors.

The estimates of relative standard deviations of fraction concentrations of air ions in the region of large ions show quite a good agreement with those of aerosol measurements in a diameter interval of 10–100 nm [Kikas et al., 1996]. According to the latter measurements, the relative standard deviation of aerosol particle concentrations has a minimum value in the size range of the accumulation mode, 100–300 nm, and rises in the flanks. This is also in accord with model calculations of deposition velocities of aerosol particles [Jaenicke, 1982, 1984; Hoppel et al., 1990].

Normally, the positive air ion spectrum has a mode in a mobility range of 1.0–1.3 $cm^2 V^{-1} s^{-1}$ or 1.3–1.6 $cm^2 V^{-1} s^{-1}$, and the negative ion spectrum, in a mobility range of 1.3–1.6 $cm^2 V^{-1} s^{-1}$ or 1.6–2.0 $cm^2 V^{-1} s^{-1}$. Sometimes the "low mobility mode" of 1.0–1.3 $cm^2 V^{-1} s^{-1}$ becomes dominant in the negative ion spectrum, and the mobility spectrum of negative small ions expands over a wider region as compared to positive ions. The mode of positive ion spectrum only shifts from mobilities of 1.3–1.6 $cm^2 V^{-1} s^{-1}$ to 1.0–1.3 $cm^2 V^{-1} s^{-1}$. These variations could explain the higher relative standard deviation of the big cluster ion concentration of negative polarity compared with the ions of positive polarity.

The low-mobility modes of small air ions of both polarities were recorded when the large ion concentration was decreasing, but not vice versa. The low concentration of heavy large ions allows small air ions to evolve (grow) toward clusters of large sizes, and consequently to lower mobilities, within their lifetime. The evolution of the mobility spectra of small air ions described above was more regular in the warm season under conditions of anticyclones, particularly in June and August. In June and August, under conditions of hot and sunny anticyclonic weather, the low-mobility mode of negative ions in a mobility range of 1.0–1.3 $cm^2 V^{-1} s^{-1}$ preferentially became dominant in the afternoon (or in the evening) and disappeared before sunset.

Considering the whole data set, the fractions of small ions of mobilities of 1.0–1.3 $cm^2 V^{-1} s^{-1}$ and 1.3–1.6 $cm^2 V^{-1} s^{-1}$ are the most conservative; the fractions of higher or lower mobility show higher relative standard deviations. Accordingly, the mobility of 1.3 $cm^2 V^{-1} s^{-1}$ (diameter of 0.88 nm) may be used as a conventional boundary between small and big cluster ions. The fractions of negative small cluster ions at daytime display almost equal variabilities.

In general, small air ion concentrations have higher relative standard deviations in the nighttime than in the daytime, because of higher concentrations raised during nocturnal calms, in fine weather conditions in the warm season. The highest relative standard deviations of small cluster ion concentration were recorded in July in conditions of very hot and stable anticyclones, probably due to increasing ionization rate caused by accumulation of radon, thoron, and their daughters near the ground during nocturnal calms that produced numerous new young ions. The higher the mobility of small cluster ions, the higher the relative standard deviation was: for example, 40% for the ions of 1.3–1.6 $cm^2 V^{-1} s^{-1}$ and 60% for the ions of 2.5–3.14 $cm^2 V^{-1} s^{-1}$.

### 3.2. Average Characteristics and Variability of Main Ion Groups

***3.2.1. Small ions.*** The statistical characteristics of small air ion concentrations are presented in Table 2. The average concentrations of small air ions and their standard deviations are $n_- = 245 \pm 88$ $cm^{-3}$ and $n_+ = 274 \pm 96$ $cm^{-3}$.

Table 2. Statistics of Negative/Positive Small Ion Concentrations ($cm^{-3}$)

| Mobility, $cm^2 V^{-1} s^{-1}$ | Mean | Median | Maximum | Lower Quartile | Upper Quartile | Relative s.d. |
|---|---|---|---|---|---|---|
| 2.51–3.14 | 12/7 | 10/7 | 67/42 | 8/5 | 13/8 | 0.45/0.51 |

| | | | | | | |
|---|---|---|---|---|---|---|
| 2.01–2.51 | 33/19 | 29/17 | 180/99 | 24/14 | 37/23 | 0.41/0.44 |
| 1.60–2.01 | 56/45 | 51/41 | 265/207 | 44/34 | 62/51 | 0.37/0.38 |
| 1.28–1.60 | 59/69 | 55/64 | 252/303 | 44/54 | 68/79 | 0.36/0.35 |
| 1.02–1.28 | 42/69 | 40/66 | 157/284 | 28/54 | 54/83 | 0.44/0.36 |
| 0.79–1.02 | 24/41 | 21/39 | 107/154 | 12/29 | 33/51 | 0.59/0.40 |
| 0.63–0.79 | 13/16 | 11/14 | 83/74 | 6/10 | 18/21 | 0.68/0.50 |
| 0.50–0.63 | 8/8 | 6/7 | 58/45 | 4/5 | 9/10 | 0.72/0.59 |
| 0.50–3.14 | 245/274 | 231/259 | 990/1167 | 183/210 | 290/319 | 0.36/0.35 |
| 1.28/1.00–3.14 | 159/209 | 148/196 | 737/928 | 124/162 | 178/238 | 0.37/0.35 |
| 0.50–1.28/1.00 | 86/65 | 78/61 | 361/239 | 50/44 | 115/82 | 0.51/0.43 |

Number of measurements: 8615.

The correlation coefficient between the polar concentrations is 98%. The mean natural mobility of small air ions of both polarities is calculated by averaging over the mobility interval from 0.5 to 3.2 $cm^2\ V^{-1}\ s^{-1}$. The hourly mean mobilities and standard deviations, averaged over the whole measurement period of 14 months, are $k_- = 1.53 \pm 0.10$ and $k_+ = 1.36 \pm 0.06\ cm^2\ V^{-1}\ s^{-1}$. Approximately the same values of mean mobility have been found for different annual periods from 1985 to 1994. The correlation coefficient between polar mean mobilities is 80%. The mean mobility of small ions reduced to standard conditions is not discussed here because of the complicated nonlinear character of the reduction procedure [Tammet, 1998].

The frequency distributions of the concentration of positive small ion categories (original fractions $P_1$–$P_8$, classes of small and big clusters and their total concentration) are approximately lognormal and can be derived from the moments of distribution presented in Table 2. In the case of positive small cluster ions, the distribution of the largest extreme gives a closer approximation, and in the case of big cluster ions, the gamma distribution is closer. The concentration of negative small cluster ions behaves similarly, but the concentration of negative big cluster ions shows different character. Its frequency distribution is extremely asymmetric, with a maximum at about 45 $cm^{-3}$, below the lower quartile (see Table 2).

The observed average values of mean mobility are comparable with those found by Dhanorkar and Kamra [1992], 1.37 and 1.25 $cm^2\ V^{-1}\ s^{-1}$ for negative and positive polarity, respectively. The average values of reduced mobility at STP, as reported by Mohnen [1977], are 1.24 and 1.14 $cm^2\ V^{-1}\ s^{-1}$ for negative and positive polarity, respectively. In both cases the ratio of negative to positive mobility is about 1.1.

The mean natural mobility of small air ions is higher in winter than in summer. The averaged mean mobility values and their standard deviations recorded in December and May are $k_{-Dec} = 1.63 \pm 0.09\ cm^2\ V^{-1}\ s^{-1}$, $k_{+Dec} = 1.41 \pm 0.04\ cm^2\ V^{-1}\ s^{-1}$ and $k_{-May} = 1.47 \pm 0.09\ cm^2\ V^{-1}\ s^{-1}$, $k_{+May} = 1.32 \pm 0.05\ cm^2\ V^{-1}\ s^{-1}$. An analogous difference of mobilities was also found formerly [Hõrrak et al., 1994].

The average negative and positive polar conductivities are nearly equal; that can be explained by the relatively high position (5 m) of air inlet and the screening of the electric field by trees surrounding the building where the instrumentation is located. The average polar conductivities calculated according to the entire measured mobility interval of 0.00032–3.2 $cm^2\ V^{-1}\ s^{-1}$ are $l_- = 6.18 \pm 2.14\ fS\ m^{-1}$ and $l_+ = 6.18 \pm 2.14\ fS\ m^{-1}$. These polar conductivities are nearly equal with those of small ions $l_{-S} = 5.96 \pm 2.11\ fS\ m^{-1}$ and $l_{+S} = 5.97 \pm 2.11\ fS\ m^{-1}$; the increased average mobility of negative small ions as compared to that of positive ions entirely compensates differences in the concentration, on average. The ratio of positive ion concentration to that of negative ions (coefficient of unipolarity) is $1.127 \pm 0.074$, and the ratio of the average mobility of negative ions to that of positive ions is $1.124 \pm 0.049$. A regression analysis shows that the polar total conductivities are nearly equal; considering the entire range of measured values of conductivities from about 1.5 to 26 $fS\ m^{-1}$, the correlation coefficient is 99%. The conductivity (also small ion concentration) underwent decrease since 1985–1986 from about 9 $fS\ m^{-1}$ to 6 $fS\ m^{-1}$ in 1993–1994.

In fine weather conditions, both the mean mobility and the total concentration of small ions have the average diurnal variation of a single wave shape with a maximum in the nighttime and a minimum in the afternoon [Hõrrak et al., 1998b]. The concentration of small ions has some considerable diurnal variation only in the warm season when the soil

is unfrozen. The average diurnal variation of negative small ions is caused mainly by small cluster ions.

The absolute maximum of the total concentration of small ions recorded on August 26 was 996 $cm^{-3}$ for negative ions and 1176 $cm^{-3}$ for positive ions, both in early morning hours (0830 LST) in fine weather conditions. The origin of the high concentrations was probably the accumulation of radon and thoron near the ground during nocturnal calms. Daytime minimum values were 239 $cm^{-3}$ for negative ions and 269 $cm^{-3}$ for positive ions. The absolute maxima were recorded at the end of a 3-day period of very weak winds at daytime and calm in the nighttime. The highest concentration of the high-mobility fraction of small cluster ions (2.51–3.14 $cm^2 V^{-1} s^{-1}$) was also recorded in the same morning at 0830 LST, when the negative ion concentration was 65 $cm^{-3}$ and the positive ion concentration was 38 $cm^{-3}$. The minimum values recorded on the same day at the afternoon were about 10 $cm^{-3}$ and 5 $cm^{-3}$ for negative ions and positive ions, respectively. This means that during nighttime and early morning hours there exists some amount of very young ions with mobilities higher than 3.14 $cm^2 V^{-1} s^{-1}$ generated by the radioactivity of radon and thoron and their daughters. These ions remain out of scope of the mobility spectrometers. At other times their concentration is comparable with the measurement uncertainties. The largest contribution of the fraction (2.51–3.14 $cm^2 V^{-1} s^{-1}$) to the total concentration of polar small ions was 7% and 4% for negative ions and positive ions, respectively. The estimated amount of high-mobility cluster ions (higher than 3.14 $cm^2 V^{-1} s^{-1}$) during nighttime and early morning hours was about 2 times less than the above mentioned 7% and 4% from the total polar concentration of small ions for negative ions and positive ions, respectively.

Table 3. Statistics of the Negative/Positive Intermediate Ion Concentrations ($cm^{-3}$)

| Mobility, $cm^2 V^{-1} s^{-1}$ | Mean | Median | Maximum | Lower Quartile | Upper Quartile | Relative s.d. |
|---|---|---|---|---|---|---|
| 0.40–0.50 | 5/5 | 4/5 | 49/48 | 3/3 | 6/6 | 0.82/0.73 |
| 0.32–0.40 | 3/4 | 2/3 | 52/37 | 1/2 | 4/5 | 1.15/0.80 |
| 0.25–0.32 | 3/2 | 2/2 | 56/42 | 1/1 | 3/3 | 1.21/1.10 |
| 0.150–0.293 | 8/7 | 5/5 | 155/116 | 4/4 | 8/7 | 1.19/1.08 |
| 0.074–0.150 | 12/12 | 8/8 | 279/250 | 6/6 | 12/12 | 1.28/1.23 |
| 0.034–0.074 | 25/25 | 18/18 | 447/437 | 14/14 | 25/25 | 1.14/1.16 |
| 0.034–0.50 | 57/55 | 40/41 | 1008/874 | 31/32 | 58/57 | 1.08/1.03 |
| 0.25–0.50 | 11/12 | 9/10 | 157/116 | 6/7 | 13/13 | 0.95/0.78 |
| 0.034–0.293 | 45/44 | 31/31 | 851/761 | 24/24 | 45/44 | 1.14/1.13 |

***3.2.2. Intermediate ions.*** The statistical characteristics of intermediate ion concentrations are presented in Table 3. The average concentration of intermediate ions is relatively low, about 50 $cm^{-3}$, but occasionally very high concentrations are recorded owing to the bursts of intermediate ions with concentrations of up to 900 $cm^{-3}$ [Hõrrak et al., 1998b]. The bursts occurred around local noon, the enhanced concentrations were recorded from 1000 to 1900 LST, with a duration of 6–10 hours, in fine weather conditions. The correlation coefficient between the total concentrations of positive and negative intermediate ions is 97%.

A burst of intermediate ions can initiate a process of the evolution of aerosol ions generating new aerosol particles that grow toward large sizes. This process looks like a triggering of a nucleation process with the accumulation of particles in the nucleation mode size range of 9.7–15 nm. Besides the process of evolution, a process of another character was also observed: a spectral mode suddenly appeared in the nucleation size range of 9.7–15 nm (mobility range of 0.0091–0.021 $cm^2 V^{-1} s^{-1}$) or 15–22 nm (0.0042–0.091 $cm^2 V^{-1} s^{-1}$) and remained there for 4–8 hours (during the time of intensive sunlight), slightly changing in height. Several such events have been observed when an anticyclonic air mass of good visibility has come over the Baltic Sea to inland areas. In general the disturbed region of air ion mobility spectra affected by the bursts of intermediate ions was observed from about 0.002 to 1.0 $cm^2 V^{-1} s^{-1}$ (from 1.1 to 34 nm), including the groups of big cluster ions and light large ions.

In contrast to the light intermediate ions (0.32–0.50 $cm^2 V^{-1} s^{-1}$), the fraction concentrations of which are nearly

equal, the heavy intermediate ions (0.034–0.293 cm V s ) show a rise in concentration toward lower mobilities. During the days with intermediate ion bursts, the ratio of concentrations of heavy to light fraction varies from about 3 to 7. The frequency distributions of the concentration of light intermediate ion fractions are asymmetric, approximately lognormal, because of the burst events. The concentrations of heavy intermediate ion fractions are roughly lognormally distributed because of extremely high values recorded during the burst events.

In order to present some statistical description of the bursts of intermediate ions, the number of days in the month when the concentration of intermediate ions is higher than a certain value is given in Table 4. Only more pronounced burst events are considered, when the intermediate ion polar concentration exceeds 100 $cm^{-3}$ (background of about 50 $cm^{-3}$) during at least 2 hours. Commonly, the burst duration was 6–10 hours (from background up to maximum and down to background). The bursts of shorter duration are marked by an asterisk in Table 4. The same is also true for intermediate ions of negative polarity, but sometimes during the burst events, peak values of the concentration of negative intermediate ions exceed those of positive polarity by about 100–150 $cm^{-3}$.

Table 4. Number of Days in the Month When the Concentration of Positive Intermediate Ions Exceeds a Certain Value

| | | >100 $cm^{-3}$ | >200 $cm^{-3}$ | >300 $cm^{-3}$ | >400 $cm^{-3}$ | >500 $cm^{-3}$ | >600 $cm^{-3}$ | Maximum $cm^{-3}$ |
|---|---|---|---|---|---|---|---|---|
| Sept. | 1993 | 13 | 8 | 3 | 0 | 0 | 0 | 381 |
| Oct. | 1993 | 8 | 8 | 7 | 5 | 1 | 1* | 874 |
| Nov. | 1993 | 5 | 3 | 3 | 0 | 0 | 0 | 442 |
| Dec. | 1993 | 2 | 1 | 1 | 1* | 0 | 0 | 457 |
| Jan. | 1994 | 1 | 1 | 1 | 1* | 0 | 0 | 471 |
| Feb. | 1994 | 2 | 2 | 2 | 2 | 2 | 1 | 601 |
| March | 1994 | 8 | 6 | 3 | 2 | 1 | 1 | 708 |
| April | 1994 | 5 | 2 | 2 | 2 | 1 | 1 | 860 |
| May | 1994 | 18 | 12 | 7 | 6 | 4 | 1 | 712 |
| June | 1994 | 11 | 6 | 2 | 1 | 0 | 0 | 470 |
| July | 1994 | 5 | 1* | 0 | 0 | 0 | 0 | 205 |
| Aug. | 1994 | 6 | 1 | 0 | 0 | 0 | 0 | 205 |
| Sept. | 1994 | 6 | 2 | 2 | 1 | 1 | 0 | 506 |
| Oct. | 1994 | 11 | 6 | 3 | 2 | 1 | 1 | 652 |
| | Sum | 101 | 59 | 36 | 23 | 11 | 6 | |

* Burst of short duration: October and December within 2 hours, January within 3 hours more than 100 $cm^{-3}$.

In the period from November 24 to February 24, only three bursts were recorded, and even those bursts were of short duration, being higher than 100 $cm^{-3}$ for only 2–3 hours. This is probably due to the fact that the conditions in winter did not favor photochemical nucleation because of low solar radiation intensity and duration at this latitude. There may also be a low concentration of nucleating low-pressure vapors. Also the decreasing mixing rate of the boundary layer and the accumulation of aerosol pollutants may be responsible for the absence of burst events in wintertime.

Regular bursts started as early as February 25 and 26, when bursts up to 600 $cm^{-3}$ were recorded. The higher concentrations in May could be related to the beginning of the period of early vegetation and intensive agricultural works. On the basis of the side-by-side measurements of aerosol particle size spectra [Hõrrak et al., 1996, 1998a] it can be concluded that the period of intensive bursts of intermediate ions followed the inflow of cool and clean high-pressure air mass. This inflow occurred on May 1, when the concentration of particles in the accumulation size range (100–560 nm) decreased rapidly from about 2400 $cm^{-3}$ to 100 $cm^{-3}$ and, after that, started gradually to increase again.

J. Mäkelä (personal communication, 1998) and Birmili [1998] have found the same regularities: the low concentration of ultrafine aerosol particles below 10 nm during wintertime and bursts in spring. The number of days

with nucleation events of 3–5 nm particles observed at Hyytiälä forest station, southern Finland, was 56 during a 1-year period in 1996–1997 (J. Mäkelä, personal communication, 1998). This number has the same order of magnitude as the number of bursts of intermediate ions, about 80, for a 1-year period at Tahkuse in 1993–1994. The number of nucleation events found by Birmili [1998] in central Europe, near Leipzig, was between 38 and 60 during different seasons in 1996–1997.

3.2.3. Large ions. The statistical characteristics of large ion concentrations are presented in Table 5.

Table 5. Statistics of the Negative/Positive Large Ion Concentration ($cm^{-3}$)

| Mobility, $cm^2\ V^{-1}\ s^{-1}$ | Mean | Median | Maximum | Lower Quartile | Upper Quartile | Relative s.d. |
|---|---|---|---|---|---|---|
| 0.0016–0.034 | 42/45 | 30/34 | 806/810 | 23/25 | 44/46 | 1.07/1.03 |
| 0.0091–0.0205 | 97/96 | 74/74 | 1673/1684 | 53/53 | 107/107 | 0.93/0.97 |
| 0.0042–0.0091 | 162/157 | 139/128 | 1874/1852 | 96/91 | 187/182 | 0.73/0.79 |
| 0.00192–0.0042 | 282/282 | 252/251 | 2139/2172 | 177/171 | 343/344 | 0.58/0.60 |
| 0.00087–0.00192 | 463/493 | 433/460 | 2604/2626 | 294/321 | 595/627 | 0.50/0.47 |
| 0.00041–0.00087 | 609/610 | 567/562 | 3119/3311 | 380/380 | 787/792 | 0.51/0.50 |
| 0.00041–0.034 | 1655/1783 | 1540/1578 | 8057/8099 | 1097/1116 | 2068/2103 | 0.48/0.47 |
| 0.0042–0.034 | 301/297 | 245/238 | 4276/4279 | 179/168 | 339/336 | 0.80/0.84 |
| 0.00041–0.0042 | 1354/1385 | 1258/1295 | 6881/6908 | 883/910 | 1720/1751 | 0.47/0.47 |

As compared with intermediate ions, the frequency distributions of the concentration of light large ion categories (original fractions 15–17 and their total concentration) are closer to lognormal. As an exception, the frequency distribution of the fifteenth fraction shows similarity to that of intermediate ions. In all cases the frequency distributions are asymmetric because of high
outliers. The frequency distributions of the concentration of heavy large ion categories (original fractions 18–20 and total concentration) are close to gamma distribution. There is no substantial difference between large ions of negative and positive polarity.

The whole range of large ions 0.00041–0.034 $cm^2\ V^{-1}\ s^{-1}$ (diameters of 7.4–79 nm) can be divided into two classes with mobilities of 0.0042–0.034 $cm^2\ V^{-1}\ s^{-1}$ (7.4–22 nm) and 0.00041–0.0042 $cm^2\ V^{-1}\ s^{-1}$ (22–79 nm) called, by convention, light large ions and heavy large ions, respectively. In general, the ratio of concentrations of light large and heavy large ions is low, about 0.2, but in some cases (nucleation events) the ratio may be extremely high, up to about 2.5. These two categories show different behavior in the case of bursts of intermediate ions, when enhanced concentrations of light large ions have also been recorded. As a rule, the concentration of heavy large ions decreases before the burst of intermediate ions [Hõrrak et al., 1998b].

Examining the time series of heavy large ion concentration, it was found that besides short time variations (bursts with duration of less than 1 day), this fraction also has a variation of 4–6 days (typical synoptical period) and even long time trends (1–2 weeks or more). The short time variations have higher amplitudes of 2000–4000 $cm^{-3}$, that is, about 10 times higher than the amplitude of average diurnal variation. The average diurnal variation is weak, about 150 $cm^{-3}$, with a minimum in the afternoon at 1300–1400 LST. The short time variations are probably caused by pollutant transport processes. Considering cold and warm seasons separately, the average diurnal variations display different behavior. In the cold season, minimum concentrations of about 1000 $cm^{-3}$ were recorded in early morning hours at 0600–0700 LST, and maximum concentrations of about 1400 $cm^{-3}$ were recorded in late evening at 2100 LST. In the warm season, minimum concentrations of about 1200 $cm^{-3}$ were recorded in the afternoon at 1500 LST, and maximum concentrations of about 1400 $cm^{-3}$ were recorded in early morning hours at 0700 LST.

Koutsenogii [1997] concluded that submicron particles with modal diameter of 170 nm represent regional and global aerosols. Such particles have the longest residence time of about 10 days and can be transported over distances of up to 8000 km. The heavy large ions as particles with diameters of 23–80 nm have residence times of 1.5–6 days [Jaenicke, 1982]; they are transported by air masses, are accumulated in the atmosphere, and are removed from the atmosphere preferentially by precipitation and thermal diffusion. The estimates of decay constants (similar to the residence times) given by Hoppel et al. [1990] for marine boundary layer are considerably smaller, about 10–30 hours, considering

diameters of 20–80 nm. The latter estimates also take into account the loss of particles in cloud processes.

The average diurnal variation of the concentration of light large ions is similar to that of intermediate ions during the burst events, but their maximum is recorded with some time lag [Hõrrak, 1998b]. The time lag is explained by the growth of generated new particles toward larger sizes. At other times, their diurnal variation is weak and close to that of heavy large ions.

### 3.3. Statistical Classification of Air Ions According to Their Mobilities

**3.3.1. Principal component and factor analysis.** The principal component analysis (PCA), known in multivariate mathematical statistics, is applied to detect the structure of the air ion mobility spectrum, e.g., for the search of mobility boundaries between different groups of air ions. Fraction concentrations of a mobility spectrum of air ions may be interpreted as a set of variables that are closely correlated (see Table 6).

Table 6. Correlation Coefficients (in Percent) Between Negative Air Ion Mobility Fractions, September 1, 1993, to October 27, 1994

| | $N_1$ | $N_2$ | $N_3$ | $N_4$ | $N_5$ | $N_6$ | $N_7$ | $N_8$ | $N_9$ | $N_{10}$ | $N_{11}$ | $N_{12}$ | $N_{13}$ | $N_{14}$ | $N_{15}$ | $N_{16}$ | $N_{17}$ | $N_{18}$ | $N_{19}$ | $N_{20}$ |
|---|---|---|---|---|---|---|---|---|---|---|---|---|---|---|---|---|---|---|---|---|
| $N_1$ | 100 | 85 | 76 | 62 | 38 | 24 | 19 | 13 | 12 | 3 | 13 | 12 | 7 | 2 | -4 | 3 | 4 | -5 | -8 | -8 |
| $N_2$ | 85 | 100 | 93 | 80 | 51 | 31 | 23 | 11 | 6 | -4 | 9 | 8 | 1 | -8 | -16 | -11 | -11 | -18 | -22 | -24 |
| $N_3$ | 76 | 93 | 100 | 92 | 65 | 41 | 28 | 15 | 5 | -4 | 5 | 4 | -4 | -12 | -19 | -17 | -17 | -21 | -29 | -35 |
| $N_4$ | 62 | 80 | 92 | 100 | 88 | 70 | 56 | 36 | 22 | 6 | 12 | 12 | 1 | -7 | -14 | -11 | -14 | -22 | -36 | -48 |
| $N_5$ | 38 | 51 | 65 | 88 | 100 | 94 | 82 | 61 | 41 | 21 | 24 | 24 | 13 | 6 | -2 | 1 | -2 | -17 | -35 | -55 |
| $N_6$ | 24 | 31 | 41 | 70 | 94 | 100 | 93 | 73 | 51 | 28 | 32 | 32 | 20 | 13 | 5 | 9 | 5 | -13 | -32 | -52 |
| $N_7$ | 19 | 23 | 28 | 56 | 82 | 93 | 100 | 82 | 63 | 40 | 44 | 44 | 33 | 26 | 17 | 20 | 15 | -4 | -23 | -42 |
| $N_8$ | 13 | 11 | 15 | 36 | 61 | 73 | 82 | 100 | 72 | 54 | 56 | 57 | 48 | 42 | 34 | 35 | 30 | 13 | -5 | -23 |
| $N_9$ | 12 | 6 | 5 | 22 | 41 | 51 | 63 | 72 | 100 | 66 | 66 | 68 | 63 | 59 | 52 | 50 | 44 | 29 | 12 | -5 |
| $N_{10}$ | 3 | -4 | -4 | 6 | 21 | 28 | 40 | 54 | 66 | 100 | 69 | 71 | 66 | 60 | 52 | 46 | 40 | 31 | 18 | 5 |
| $N_{11}$ | 13 | 9 | 5 | 12 | 24 | 32 | 44 | 56 | 66 | 69 | 100 | 97 | 87 | 73 | 58 | 43 | 34 | 22 | 10 | 1 |
| $N_{12}$ | 12 | 8 | 4 | 12 | 24 | 32 | 44 | 57 | 68 | 71 | 97 | 100 | 89 | 75 | 58 | 43 | 33 | 20 | 9 | 0 |
| $N_{13}$ | 7 | 1 | -4 | 1 | 13 | 20 | 33 | 48 | 63 | 66 | 87 | 89 | 100 | 92 | 78 | 61 | 47 | 34 | 19 | 6 |
| $N_{14}$ | 2 | -8 | -12 | -7 | 6 | 13 | 26 | 42 | 59 | 60 | 73 | 75 | 92 | 100 | 93 | 77 | 62 | 47 | 29 | 13 |
| $N_{15}$ | -4 | -16 | -19 | -14 | -2 | 5 | 17 | 34 | 52 | 52 | 58 | 58 | 78 | 93 | 100 | 88 | 77 | 65 | 44 | 23 |
| $N_{16}$ | 3 | -11 | -17 | -11 | 1 | 9 | 20 | 35 | 50 | 46 | 43 | 43 | 61 | 77 | 88 | 100 | 92 | 78 | 54 | 31 |
| $N_{17}$ | 4 | -11 | -17 | -14 | -2 | 5 | 15 | 30 | 44 | 40 | 34 | 33 | 47 | 62 | 77 | 92 | 100 | 90 | 70 | 46 |
| $N_{18}$ | -5 | -18 | -21 | -22 | -17 | -13 | -4 | 13 | 29 | 31 | 22 | 20 | 34 | 47 | 65 | 78 | 90 | 100 | 89 | 66 |
| $N_{19}$ | -8 | -22 | -29 | -36 | -35 | -32 | -23 | -5 | 12 | 18 | 10 | 9 | 19 | 29 | 44 | 54 | 70 | 89 | 100 | 87 |
| $N_{20}$ | -8 | -24 | -35 | -48 | -55 | -52 | -42 | -23 | -5 | 5 | 1 | 0 | 6 | 13 | 23 | 31 | 46 | 66 | 87 | 100 |

The absolute value of critical correlation coefficient at a confidence level of 95% is 3%.

The formal correlation is caused by the following: (1) physical and chemical processes embracing a group of fractions (causing positive correlation) or acting between different groups of fractions (causing opposite correlation) and (2) unavoidable smoothing of a spectrum due to the finite resolution of the measuring apparatus. The information about variance and covariance, which is included in different fractions of a mobility spectrum, can be transferred by a considerably smaller number of new variables, called principal components or factors, which are proper linear combinations of original variables. The search for principal components reduces to a search for eigenvalues (characteristic roots, portions of common variance explained by factors) and factor loadings (characteristic vectors) of a correlation matrix of original variables.

Before performing PCA, the original variables (fractions of air ion mobility spectra) were treated with a nonlinear transformation by logarithmic scaling. This procedure transforms asymmetric frequency distributions of variables closer to the normal ones, assumed by PCA. The logarithmic scaling does not significantly affect the results of the

classification of air ions in our case. Finally, the variables were standardized to provide variables of a comparable variance. To obtain a clear pattern ("simple structure") of loadings, the VARIMAX rotation, often used in factor analysis, has been performed herein.

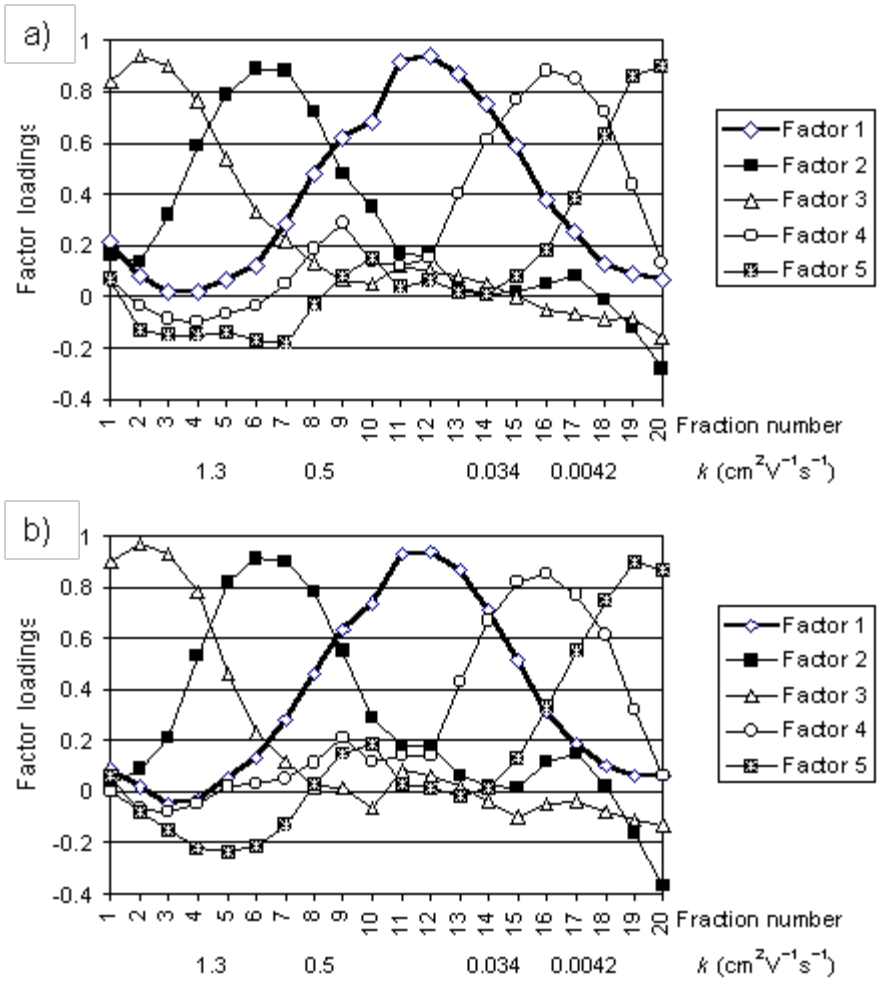


Figure 5. Factors of air ion mobility spectra for (a) positive ions and (b) negative ions. The mobility and diameter boundaries of fractions are given in Table 1.

The eigenvalue problem was solved separately for the correlation matrices of logarithmically rescaled and standardized variables of positive and negative ions (Table 6). There is some clear structure in these correlation matrices. Results are presented in Figure 5 for positive and negative ions, respectively. The boundaries of spectral fractions and corresponding diameter intervals for single charged particles are given in Table 1.

The first five successfully extracted factors explain 92% of total variance. The total variance that can be potentially extracted is equal to the number of variables, which is 20. Each of the first five factors extracts at least as much variance as the equivalent of one original variable, i.e., 5% (it is expected that the variance of a single standardized variable is 1); a deep drop follows thereafter. The subsequent 14 factors explain only 8% of the total variance. Each of the latter factors explains less than 1.5% of the total variance. A part of this variation is caused by instrumental noise. Thus we can conclude that the mobility spectrum, in the first approximation, has 5 degrees of freedom or that the spectrum can be described almost completely by these five factors representing 92% of all measured information.

The first factor (factor 1 in Figure 5) is closely correlated with intermediate ions (fractions 9–14), and thus it can be called the "burst factor" of intermediate ions. It explains 24% of variance, more than others do. Factor 2 is closely correlated with big cluster ions (fractions 4–8); factor 3, with small cluster ions (fractions 1–4); and factor 4, with light

large ions (fractions 15–18). They explain approximately equal variances of 20%, 18%, and 17% for factors 2, 3, and 4, respectively. The contribution of factor 5, associated with heavy large ions (fractions 18–20), is the lowest, 13%. This factor also is correlated oppositely with cluster ions (fractions 2–7). In the same sense, factor 2, which is closely correlated with big cluster ions (fractions 5–8), is correlated negatively with heavy large ions (fractions 19–20).

3.3.2. Air ion classes. The study of the correlation between the factors and air ion fractions shows that all the air ions can be divided into two main classes: (1) aerosol ions with mobilities below 0.5 $cm^2 V^{-1} s^{-1}$ and (2) cluster ions with mobilities above 0.5 $cm^2 V^{-1} s^{-1}$. These two classes can in turn be divided into two classes of cluster ions (small and big cluster ions) and three classes of aerosol ions (intermediate, light, and heavy large ions). The classification, based on statistical analysis, is given in Table 7. This classification is still to a certain extent conventional, and the boundaries are not exactly determined, because the factors that were chosen as representative have cross loadings (any variable is correlated with more than one factor; see Figure 5).

Table 7. Classification of Air Ions

| Class of Air Ions | Mobility, $cm^2 V^{-1} s^{-1}$ | Diameter, nm | Traditional Name |
|---|---|---|---|
| Small cluster ions | 1.3–3.2 | 0.36–0.85 | small ions |
| Big cluster ions | 0.5–1.3 | 0.85–1.6 | small ions |
| Intermediate ions | 0.034–0.5 | 1.6–7.4 | intermediate ions |
| Light large ions | 0.0042–0.034 | 7.4–22 | large ions |
| Heavy large ions | 0.00041–0.0042 | 22–79 | large ions |

Considering the warm season (from May to September) separately from the entire period, the factor analysis revealed different boundaries between small cluster ions and big cluster ions of different polarity: negative small and big cluster ions have a boundary of 1.3 $cm^2 V^{-1} s^{-1}$, and positive ions, 1.0 $cm^2 V^{-1} s^{-1}$ (diameter of 1 nm). The mobility boundary of 1.3 $cm^2 V^{-1} s^{-1}$ halves the peak in the mobility spectrum of positive small ions (see Figure 3). If we use the boundary of 1.3 $cm^2 V^{-1} s^{-1}$ for cluster ions of both polarities, then we obtain a lower concentration of positive small cluster ions compared to negative ions, and this would be in contradiction to our understanding about the electrode effect near the ground. The use of the boundary of 1.0 $cm^2 V^{-1} s^{-1}$ for positive ions also facilitates the description of the average diurnal variation of cluster ion characteristics. Therefore we suggest the use of a boundary of 1.0 $cm^2 V^{-1} s^{-1}$ between small and big cluster ions of positive polarity instead of 1.3 $cm^2 V^{-1} s^{-1}$. However, such a specification is rather speculative; measurements of small ion mobility spectra with higher resolution are necessary to establish the boundary more precisely.

In the warm season, the boundary between light and heavy large ions is shifted to a lower mobility of 0.00192 $cm^2 V^{-1} s^{-1}$ (diameter of 34 nm) compared to that of the cold season 0.0043 $cm^2 V^{-1} s^{-1}$ (diameter of 22 nm).

The boundary mobility of 0.5 $cm^2 V^{-1} s^{-1}$ or a diameter of 1.6 nm is the same boundary, which has been considered physically as the boundary between molecular clusters and macroscopic particles [Tammet, 1995]. The same value of 0.5 $cm^2 V^{-1} s^{-1}$ was also considered as the lower boundary of small air ions formerly [Hõrrak et al., 1994].

The classification of air ions presented in Table 7 may also be obtained by PCA without the Varimax rotation procedure, using the first two factors (with respect to eigenvalues) as classifiers. In this case, at first, the boundary between cluster ions and aerosol ions can be determined more accurately when excluding the burst events of intermediate ions. The subsequent classification within separated classes of cluster ions and aerosol ions makes it possible to gradually detail the boundaries between different classes of air ions. The presented classification is in general also predictable from the average spectrum and from the relative standard deviations of fraction concentrations (see Figures 2, 3, and 4).

The above classes of air ions could be physically characterized as follows:

1. *Small cluster ions* have mobility of 1.3–2.5 $cm^2 V^{-1} s^{-1}$, estimated diameter of 0.36–0.85 nm, mass of 30–400 unified atomic mass units (u), and typical lifetime of 5–60 s. Considering ion diameters, the core of a cluster could contain one inorganic molecule and be surrounded by one layer of water molecules. After recombination, small cluster ions would be destroyed and again separated into initial components (cores and water molecules).

2. *Big cluster ions* have mobility of 0.5–1.3 $cm^2 V^{-1} s^{-1}$, estimated diameter of 0.85–1.6 nm, and mass of 400–2500 u. Considering ion diameters, the core of a cluster could contain one organic molecule and be surrounded by a layer of water molecules. The enhanced concentrations have been recorded when large ion concentration is low, which makes it possible for them to evolve to large sizes within their longer lifetime. In the case of intensive nucleation events (bursts), the enhanced concentrations were recorded simultaneously with intermediate ion concentrations. Contrary to aerosol ions, collisions between cluster ions and ambient gas molecules are considered elastic [Tammet, 1995].

3. *Intermediate ions* have mobility of 0.034–0.5 $cm^2 V^{-1} s^{-1}$ and diameter of 1.6–7.4 nm. A corresponding class of aerosol particles is the "fine nanometer particles". Some intermediate ions are a product of ion-induced nucleation: nucleating vapor condenses onto cluster ions, which grow to the size of intermediate ions, called the "primary aerosol ions". Particles born in the neutral stage in the process of gas-to-particle conversion or nucleation and charged by attachment of cluster ions are called the "secondary aerosol ions".

4. *Light large ions* have mobility of 0.0042–0.034 $cm^2 V^{-1} s^{-1}$ and diameter of 7.4–22 nm. A corresponding class of aerosol particles is the "ultrafine particles" or "coarse nanometer particles". They are single charged and often in a quasi-steady state of stochastic charging with cluster ions.

5. *Heavy large ions* have mobility of <0.0042 $cm^2 V^{-1} s^{-1}$ and diameter of >22 nm. A corresponding class of aerosol particles could be called the "Aitken particles". They are, as a rule, in a quasi-steady state of stochastic charging with cluster ions, and some of them may carry multiple charges.

We suppose that small cluster ions represent a group of young ions and big clusters represent a group of aged ions. This assumption is in accordance with the measurements of the mobility spectra of ions generated in laboratory air [Nagato and Ogawa, 1998]. They have found no ions below 0.8 $cm^2 V^{-1} s^{-1}$ in the mobility spectrum of young ions, while a considerable number of ions was observed down to 0.3 $cm^2 V^{-1} s^{-1}$ in the spectrum of natural ions. It was supposed that the cluster ions between 0.3 and 0.8 $cm^2 V^{-1} s^{-1}$ could be formed by mechanisms other than those for the ions above 0.8 $cm^2 V^{-1} s^{-1}$. Our measurements show the boundary between two groups at 1.0 $cm^2 V^{-1} s^{-1}$ and 1.3 $cm^2 V^{-1} s^{-1}$ for the ions of positive and negative polarity, respectively.

The presented classification of aerosol ions is in accord with the three-modal structure of submicron aerosol particle size distribution found in continental sites and in the Arctic marine boundary layer [Kulmala et al., 1996; Mäkelä et al., 1997; Covert et al., 1996; Birmili, 1998]. These modes have mean diameters of about 150–250 nm, 40–70 nm, and 5–14 nm and are referred to as the accumulation, Aitken, and nucleation (or ultrafine) modes, respectively. There were clear minima in number concentrations between these modes that appeared at 20–30 nm and 80–100 nm. Thus the intermediate ions (0.034–0.5 $cm^2 V^{-1} s^{-1}$, 1.6–7.4 nm) and light large ions (0.0042–0.034 $cm^2 V^{-1} s^{-1}$, 7.4–22 nm) may be classified as two classes of nucleation mode particles, and heavy large ions (0.00041–0.0042 $cm^2 V^{-1} s^{-1}$, 22–79 nm), as charged Aitken mode particles. It may be concluded that in the atmosphere, there exists a natural boundary dividing ultrafine particles at about 7.4 nm, and when studying aerosol processes, the size range of 1.6–7.4 nm can be considered the range of fine nanometer particles.

## 4. Conclusions

The average spectrum of air ions in a wide mobility range of 0.00041–3.2 $cm^2 V^{-1} s^{-1}$ is established on the ground of a statistically weighty database: 14 months, 8615 hourly averaged spectra of both polarities, and 20 logarithmically distributed fractions per spectrum. The average spectrum gives a basis for distinguishing three main air ion groups: small, intermediate, and large ions. The groups of small and large ions are distinctly seen as peaks in an average mobility spectrum. Physically, large and intermediate ions can be called aerosol ions and small ions can be called cluster ions.

Small (cluster) ions represent quite isolated and stable groups of ions with mean natural mobility and standard deviation of $1.53 \pm 0.10$ and $1.36 \pm 0.06$ $cm^2 V^{-1} s^{-1}$ for negative and positive ions, respectively. The ratio of the concentration of positive ions to that of negative ions (coefficient of unipolarity) is about 1.12, as well as the ratio of the average mobility of negative ions to that of positive ions. Accordingly, the average polar conductivities and their standard deviations, caused mainly by small ions, are equal: $\lambda_- = 6.18 \pm 2.14$ fS $m^{-1}$ and $\lambda_+ = 6.18 \pm 2.14$ fS $m^{-1}$. This can be explained by a relatively high position (5 m) of the air inlet and the screening of the electric field by trees

surrounding the building where the instrumentation is located.

The overall shape of the spectra in the range of large ions (aerosol ions) is in accord with calculations based on the theory of bipolar charging of aerosol particles by small air ions. The concentration of large ions diminishes toward higher mobilities owing to a reduction of charging probability and of the concentration of aerosol particles.

Certain thermodynamical causes hinder the growth of cluster ions in ordinary environmental conditions, keeping the concentration of intermediate ions (0.034–0.5 $cm^2 V^{-1} s^{-1}$; 1.6–7.4 nm) at a low background of about 50 $cm^{-3}$. Enhanced concentrations of intermediate ions up to about 900 $cm^{-3}$ (bursts) are observable in the mobility spectra in fine weather conditions during daytime. The number of burst events of intermediate ions recorded during 14 months was 101 (about 80 per year), with maximum frequency in spring and minimum frequency in winter. Intermediate ions are formed probably by diffusion charging of nanometer aerosol particles generated by photochemical nucleation process. At the same time, cluster ions can also grow up to intermediate ion size range. The measurements of intermediate ion mobility spectra may give essential information about nanometer particles and their electrical state in the case of nucleation events. These measurements may be used parallel to the nanometer particle measurements, in order to explain the importance of the possible routes of the generation of nanometer particles via homogeneous and ion-induced nucleation.

The relative standard deviation of the hourly averaged values of fraction concentration is about 50% for small (cluster) ions, 70% for large ions, and up to 130% for intermediate ions. The considerable variability of the concentration of intermediate ions is due to their bursts in favorable conditions during daytime. During nighttime, intermediate and large ions show nearly equal relative standard deviations of 50–60%.

The principal component analysis was applied to detect the structure of an air ion mobility spectrum, for example, for the search of mobility boundaries between different groups of air ions. The first five successfully extracted factors explain 92% of total variance. The study shows that a mobility spectrum in the range of 0.00041–3.2 $cm^2 V^{-1} s^{-1}$ (0.36–79 nm) can be divided into 5 classes: small cluster ions, big cluster ions, intermediate ions, light large ions, and heavy large ions with boundaries between them: 1.3 $cm^2 V^{-1} s^{-1}$ (diameter of 0.85 nm), 0.5 $cm^2 V^{-1} s^{-1}$ (1.6 nm), 0.034 $cm^2 V^{-1} s^{-1}$ (7.4 nm), and 0.0042 $cm^2 V^{-1} s^{-1}$ (22 nm). Thus it can be concluded that the mobility spectrum, in the first approximation, has 5 degrees of freedom or that the spectrum can be described almost completely by these five factors. The presented classification of aerosol ions is in accord with the three-modal structure of the size distribution of submicron aerosol particles.

**Acknowledgments.** This research has in part been supported by the Estonian Science Foundation through grants 3050, 3326, and 3903. The authors also thank Hilja Iher and, posthumously, Rein Sepp for their assistance in measuring.

## References

Birmili, W., Production of new ultrafine aerosol particles in continental air masses, Ph.D. thesis, 107 pp., Univ. of Leipzig, Leipzig, Germany, 1998.

Covert, D. S., A. Wiedensohler, P. Aalto, J. Heintzenberg, P. H. McMurry, and C. Leck, Aerosol number size distributions from 3 to 500 nm diameter in the Arctic marine boundary layer during summer and autumn. Tellus, 48, Ser. B, 197–212, 1996.

Dhanorkar, S., and A. K. Kamra, Measurement of mobility spectrum and concentration of all atmospheric ions with a single apparatus, J. Geophys. Res., 96, 18,671–18,678, 1991.

Dhanorkar, S., and A. K. Kamra, Relation between electrical conductivity and small ions in the presence of intermediate and large ions in the lower atmosphere, J. Geophys. Res., 97, 20,345–20,360, 1992.

Dhanorkar, S., and A. K. Kamra, Diurnal variations of the mobility spectrum of ions and size distribution of fine aerosols in the atmosphere, J. Geophys. Res., 98, 2639–2650, 1993a.

Dhanorkar, S., and A. K. Kamra, Diurnal and seasonal variations of the small-, intermediate-, and large-ion concentrations and their contributions to polar conductivity, J. Geophys. Res., 98, 14,895–14,908, 1993b.

Flagan, R. C., History of electrical aerosol measurements, Aerosol Sci. Technol., 28, 301–380, 1998.

Hoppel, W. A., and G. M. Frick, Ion–aerosol attachment coefficients and the steady-state charge distribution on aerosols in a bipolar ion environment, Aerosol Sci. Technol., 5, 1–21, 1986.

Hoppel, W. A., J. W. Fitzgerald, G. M. Frick, R. E. Larson, and E. J. Mack, Aerosol size distributions and optical properties found in the marine boundary layer over the Atlantic Ocean, J. Geophys. Res., 95, 3659–3686, 1990.

Hõrrak, U., H. Tammet, J. Salm, and H. Iher, Diurnal and annual variations of atmospheric ionisation quantities in Tahkuse (in Russian with English summary), Acta Commentat. Univ. Tartu, 824, 78–83, 1988.

Hõrrak, U., F. Miller, A. Mirme, J. Salm, and H. Tammet, Air ion observatory at Tahkuse: Instrumentation, Acta Commentat. Univ. Tartu, 880, 33–43, 1990.
Hõrrak, U., H. Iher, A. Luts, J. Salm, and H. Tammet, Mobility spectrum of air ions at Tahkuse Observatory, J. Geophys. Res., 99, 10,697–10,700, 1994.
Hõrrak, U., J. Salm, and H. Tammet, Outbursts of intermediate ions in atmospheric air, in Proceedings of the 10th Conference on Atmospheric Electricity, pp. 76–79, Soc. of Atmos. Electr. of Japan, Osaka, 1996.
Hõrrak, U., A. Mirme, J. Salm, E. Tamm, and H. Tammet, Air ion measurements as a source of information about atmospheric aerosols, J. Atmos. Res., 46(3–4), 233–242, 1998a.
Hõrrak, U., J. Salm, and H. Tammet, Bursts of intermediate ions in atmospheric air, J. Geophys. Res., 103, 13,909–13,915, 1998b.
Hõrrak, U., A. Mirme, J. Salm, E. Tamm, and H. Tammet, Study of covariations of aerosol and air ion mobility spectra at Tahkuse, Estonia, J. Aerosol Sci., 29, S849–S850, 1998c.
Israël, H., Atmospheric Electricity, Vol. 1, Isr. Program for Sci. Transl., Jerusalem, 1970.
Jaenicke, R., Physical aspects of the atmospheric aerosol. in: Chemistry of the Unpolluted and Polluted Troposphere, edited by H. W. Georgii and W. Jaeschke, pp. 341–373, D. Reidel, Norwell, Mass., 1982.
Jaenicke, R., Our knowledge about the atmospheric aerosol, in Proceedings of the 11th International Conference on Atmospheric Aerosols, Condensation and Ice Nuclei, vol. 1, pp. 99–107, Hungarian Meteorol. Service, Budapest, 1984.
Kikas, Ü., A. Mirme, E. Tamm, and T. Raunemaa, Statistical characteristics of aerosol in Baltic Sea region, J. Geophys. Res., 101, 19,319–19,327, 1996.
Kim, T. O., M. Adachi, K. Okuyama, and J. H. Seinfeld, Experimental measurement of competitive ion-induced and binary homogeneous nucleation in $SO_2/H_2O/N_2$ mixtures, Aerosol Sci. Technol., 26, 527–543, 1997.
Kim, T. O., T. Ishida, M. Adachi, K. Okuyama, and J. H. Seinfeld, Nanometer–sized particle formation from $NH_3/SO_2/H_2O$/air mixtures by ionizing irradiation, Aerosol Sci. Technol., 29, 111–125, 1998.
Kojima, H., Relation between intermediate ions and meteorological factors. Res. Lett. Atmos. Electr., 4, 49–53, 1984.
Koutsenogii, P., Aerosol measurements in Siberia, J. Atmos. Res., 44, 167–173, 1997.
Kulmala, M., A. Laaksonen, P. Aalto, T. Vesala, and L. Pirjola, Formation, growth, and properties of atmospheric aerosol particles and cloud droplets, Geophysica, 32(1–2), 217–233, 1996
Luts, A., Mathematical simulation of the evolution or air ions, Ph.D. thesis, 150 pp., Univ. of Tartu, Tartu, Estonia, 1995.
Luts, A., and J. Salm, Chemical composition of small atmospheric ions near the ground, J. Geophys. Res., 99, 10,781–10,785, 1994.
Mäkelä, J. M., P. Aalto, V. Jokinen, T. Pohja, A. Nissinen, S. Palmroth, T. Markkanen, K. Seitsonen, H. Lihavainen, and M. Kulmala, Observations of ultrafine aerosol particle formation and growth in boreal forest, Geophys. Res. Lett., 24, 1219–1222, 1997.
Misaki, M., Studies of the atmospheric ion spectrum (I), Pap. Meteorol. Geophys., 12, 247–260, 1961a.
Misaki, M., Studies of the atmospheric ion spectrum (II), Pap. Meteorol. Geophys., 12, 261–276, 1961b.
Misaki, M., Mobility spectrums of large ions in the New Mexico semidesert, J. Geophys. Res., 69, 3309–3318, 1964.
Misaki, M., Measurements of atmospheric electricity (in Japanese), Kisho Kenkyu Noto, 130, 105–118, 1976.
Misaki, M., M. Ohtagaki, and I. Kanazawa, Mobility spectrometry of the atmospheric ions in relation to atmospheric pollution, Pure Appl. Geophys., 100, 133–145, 1972.
Mohnen, V. A., Formation, nature and mobility of ions of atmospheric importance, in Electrical Processes in Atmospheres, edited by H. Dolezalek and R. Reiter, pp. 1–17, Dietrich Steinkopff Verlag, Darmstadt, Germany, 1977.
Nagato, K., and T. Ogawa, Evolution of tropospheric ions observed by an ion mobility spectrometer with a drift tube, J. Geophys. Res., 103, 13,917–13,925, 1998.
Reischl, G. P., J. M. Mäkelä, R. Karch, and J. Necid, Bipolar charging of ultrafine particles in the size range below 10 nm, J. Aerosol Sci., 27, 931–949, 1996.
Salm, J., The average mobility spectrum of large ions of the troposphere, Res. Lett. Atmos. Electr., 8, 21–24, 1988.
Tammet, H., The Aspiration Method for the Determination of Atmospheric-Ion Spectra, Isr. Program for Sci. Transl., Jerusalem. 1970.
Tammet, H., A piecewise linear model of spectrum for the measurement of air ions and aerosols (in Russian with English summary), Acta Commentat. Univ. Tartu, 534, 45–54, 1980.
Tammet, H., Air ion observatory at Tahkuse: Software, Acta Commentat. Univ. Tartu, 880, 44–51, 1990.
Tammet, H., Size and mobility of nanometer particles, clusters and ions, J. Aerosol Sci., 26, 459–475, 1995.
Tammet, H., Reduction of air ion mobility to standard conditions, J. Geophys. Res., 103, 13,933–13,937, 1998.
Tammet, H., F. Miller, E. Tamm, T. Bernotas, A. Mirme, and J. Salm, Apparatus and methods for the spectrometry of small air ions (in Russian with English summary), Acta Commentat. Univ. Tartu, 755, 18–28, 1987.